ELSEVIER

Journal of Nuclear Materials 318 (2003) 84–91

journal of nuclear materials

www.elsevier.com/locate/jnucmat

R & D on mercury target pitting issue

K. Kikuchi *, H. Kogawa, M. Futakawa, S. Ishikura, M. Kaminaga, R. Hino

Japan Atomic Energy Research Institute, Tokai-mura, Ibaraki-ken 319-1195, Japan

Abstract

A technical issue in mercury spallation target development is pitting, which appears on the target vessel in conjunction with the pressure wave. Pitting has been found in off-beam line test by split Hopkinson pressure bar (SHPB) test as well as in the on-beam test of mercury target at WNR of LANSCE. In SHPB tests pressure in mercury was reduced from 80 to 40, 20 and 10 MPa. Specimens made of type 316 stainless steel were inspected before and after the impacting test at ×450 magnification. Results show that over 20 MPa pitting was generated. But at the lowest pressure in mercury, the number of pits was very limited and substantial damage was small. Substantial damage by pitting is characterized by holes where mass is removed from the wall. Depression itself may not be a substantial damage as long as it is not accompanied by holes.

1. Introduction

In R & D for high intensity spallation neutron sources, pitting has become a new technical issue for estimating the lifetime of mercury target vessels. A sub-μs short-pulsed proton beam is favored for a high intensity neutron source based on the spallation process. Currently liquid mercury is the choice of target material for a potential supply of several mega-watts of proton beam power because of the absence of damage from proton and neutron irradiations. A main technical concern for design of mercury target vessel was pressure wave effects. The ASTE collaboration [1] has been conducted to investigate the intensity of pressure waves by using a pulsed proton beam at AGS since 1997.

Irradiation damage, corrosion and fatigue in the target shell have been researched for the mercury target development. It is possible to predict the intensity of pressure waves by computer simulation [2]. However, it was recognized that for detailed analyses of target vessel response in terms of induced stress intensity and frequency, a better understanding of the interaction between mercury and target vessel was needed. It was during the research of interaction issues in the mercury target that another material issue related to mechanical damage called pitting was found. This was first seen in off-beam tests at JAERI [3] and then recognized in the real proton beam target at LANSCE by ORNL [4]. The pitting issues are strongly connected with the pressure wave. Cavitation in the mercury target is caused by beam-induced pressure waves. Bubbles grow and shrink by interaction with the surrounding mercury. When bubbles collapse near the vessel, a mercury jet flow can cause pitting on the vessel surface. The possible mechanism stated above was reported in water environment [5,6] and theoretical work was also reported [7].

Pitting damage may significantly reduce the lifetime of mercury targets, therefore current R & D issues emphasize how to mitigate the pressure wave, what will be the damage to the vessel material after over a million cycles of short pulses, and material selection to resist pitting as well as irradiation. In this report the question of a threshold value for pitting will be discussed. If material is stressed within the elastic regime, deformation of material will be recoverable and material damage will not accumulate.

* Corresponding author. Tel.: +81-29 282 5058; fax: +81-29 282 6489.

E-mail address: kikuchi@popsvr.tokai.jaeri.go.jp (K. Kikuchi).

0022-3115/03/$ - see front matter © 2003 Elsevier Science B.V. All rights reserved.
doi:10.1016/S0022-3115(03)00016-3

2. Experimental apparatus and procedure

2.1. Experimental apparatus

Fig. 1 shows the experimental apparatus used to generate on the mercury by applying the split Hopkinson pressure bar (SHPB) technique, which mainly consists of an impact bar of 300 mm length, an input bar of 1495 mm, an output bar of 1495 mm length, a collar and an air gun to shoot the impact bar. In this experiment the length of impacting bar is reduced to 300 mm from 500 mm in order to test at lower pressure regime.

Specimens of stainless steel were connected with the end of the input and output bars on the mercury side by thread set; the bottom of the specimens is to be inspected. The impact bar is 16 mm in diameter and made of the maraging steel, which has 2 GPa in yield stress to remain elastic throughout the tests. The collar is made of type 316 stainless steel is 27 mm thick of the collar. A uniaxial strain condition will be generated in the mercury by using a thick collar. The clearance between the collar and the bars is 0.05 mm. O-rings were installed between the bars and collar to prevent leakage of the mercury and to allow the stress wave to travel smoothly through the bars.

The axial length of the mercury was set to be 5 mm. The stress waves traveling in the input and output bars were measured by the strain gages set on the axial center of each bars. The gage length is 2 mm. The dynamic response of this strain measuring system is 500 kHz. Impact velocity of the impact bar, V, was measured by using two optical sensors.

2.2. Test procedure

The mercury was carefully installed inside of the collar without any air bubbles, and the length of the mercury was adjusted to be 5 mm. After finishing the setup, the impact bar was shot by the air gun to collide with the input bar and the strains on both bars were measured and stored in a digital-storage-oscilloscope (DL708;YOKOGAWA).

The incident strain is denoted by ε_i, the reflected strain by ε_r (both measured in the input bar), and the transmitted strain by ε_t (output bar).The axial stress and strain were calculated by using the Kolsky equations [8] as follows. The displacements $U_i(t)(i = 1, 2)$ at the specimen-bar interfaces are given by

$$U_1(t) = c_0 \int_0^t [-\varepsilon_i(\tau) + \varepsilon_r \tau]\, d\tau \tag{2.1}$$

on the input bar side, and

$$U_2(t) = -c_0 \int_0^t \varepsilon_t(\tau)\, d\tau \tag{2.1'}$$

on the output bar side, respectively, where c_0 is the sound velocity in the bars, E is the Young's modulus, ρ is the mass density of the bar material and t is a time. $t = 0$ indicates the time when the incident strain reaches the interface between input bar and mercury. The relative displacement of mercury between the interfaces in contact with the bars, ΔU, is given by

$$\Delta U(t) = c_0 \int_0^t [\varepsilon_i(\tau) - \varepsilon_r(\tau) - \varepsilon_t(\tau)]\, d\tau. \tag{2.2}$$

Then the average strain of the specimen, $\varepsilon(t)$, is

$$\varepsilon(t) = \frac{\Delta U(t)}{l_s}, \tag{2.3}$$

where l_s is the axial length of mercury. The loads $P_i(t)$ $(i = 1, 2)$ on the specimen ends are given by

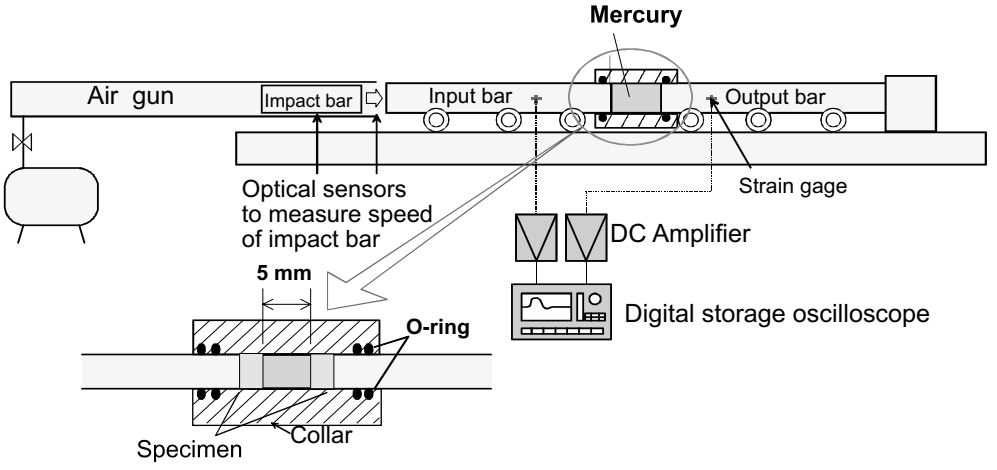

Fig. 1. Experimental apparatus for the impact incidence to the mercury using the split Hopkinson pressure bar technique.

$$P_1(t) = EA[\varepsilon_i(t) + \varepsilon_r(t)] \tag{2.4}$$

on the input bar side, and

$$P_2(t) = EA\varepsilon_t(t) \tag{2.5}$$

on the output bar side, respectively. Then the average stress in the specimen is

$$\sigma(t) = \frac{P_1(t) + P_2(t)}{2A_s} = \frac{EA}{2A_s}[\varepsilon_i(t) + \varepsilon_r(t) + \varepsilon_t(t)], \tag{2.6}$$

where E is an elastic modulus of mercury, A is a cross section of the collar and A_s is a cross section of input or output bar. In the case of $P_1(t) = P_2(t)$, the following relation is obtained from the Eqs. (2.4) and (2.5):

$$\varepsilon_i(t) + \varepsilon_r(t) = \varepsilon_t(t). \tag{2.7}$$

Therefore, the strain and stress in the specimen are given by

$$\varepsilon(t) = \frac{-2c_0}{l_s}\int_0^t \varepsilon_r(\tau)\,d\tau, \tag{2.8}$$

$$\sigma(t) = \frac{EA}{A_s}\varepsilon_t(t). \tag{2.9}$$

We measured $\varepsilon_r(t)$ and $\varepsilon_i(t)$ and estimated experimentally the relationship between the strain and the stress on the mercury by using the Eqs. (2.8) and (2.9). Assuming uniaxial strain condition in the mercury, the relationship between the pressure, P, and the stress components, σ_{ii} ($i = 1,2$ and 3) is given by

$$P = \frac{1}{3}(\sigma_{11} + \sigma_{22} + \sigma_{33}) = \sigma_{11} \tag{2.10}$$

and the relationship between the volumetric strain, $\Delta V/V$, and strain components, ε_{ii} ($i = 1$, 2 and 3) is given by

$$\Delta V/V = \varepsilon_{11} + \varepsilon_{22} + \varepsilon_{33} = \varepsilon_{11}. \tag{2.11}$$

Then the strain of the mercury, $\varepsilon(t)$, obtained by the Eq. (2.8) and the stress, $\sigma(t)$, by the Eq. (2.9) are equal to the volumetric strain of the mercury, $\Delta V/V$, and pressure, P, respectively. For a given test series the impact bar was shot at the same velocity. The mercury cavity length was carefully adjusted every shot. After 10 shots, the specimens were removed from the input and output bars to inspect by microscope. Table 1 shows the planed mercury test pressures: they are 80, 40, 20 and 10 MPa.

2.3. Specimen material and observation method

All specimens were made of type 316 austenitic stainless steel with the chemical composition 0.04C/0.47Si/1.64Mn/0.27P/0.25S/10.31Ni/16.52Cr/2.26Mo (wt%). Fig. 2 shows the specimen geometry which were machined from 18 mm diameter round bar. Specimens were polished with a final step by 1 μm diamond paste after #4000 paper. Pre-test photos were taken by microscope at ×450, a Keyence 450-ZH with 1.2M pixel resolution. The observed area is a crossed band as shown in Fig. 3.

Sixty photos were taken and stored in the computer before test. The inspected area ratio is 9% of the total surface. After test another 60 photos were taken by the

Table 1
Velocity of impacting bars and pressure in mercury

Test series number/planning pressure in mercury (MPa)	Impact bar velocity, V (m/s)	Pressure in mercury (MPa)	Average pressure in series (MPa)
1/80	5.3	79.2	83.9
	5.6	102.5	
	6.2	93.3	
	5.8	90.3	
	6.6	82.3	
	5.7	83.6	
	5.7	78.3	
	5.5	76.4	
	5.5	74.2	
	5.7	79.3	
2/40	–	–	49.0
	3.7	46	
	4.4	60.7	
	3.5	41	
	–	–	
	3.7	48.9	
	3.7	48.3	
	3.8	50	
	4.0	54.94	
	3.3	42.3	
3/20	3.1	29	25.9
	2.9	27.4	
	3.0	18.5	
	2.9	26.8	
	3.2	28.4	
	2.9	24.7	
	2.8	27.1	
	2.5	18.8	
	2.7	22.4	
	3.4	35.5	
4/10	(3.8)	(52.2)	16.8 (20.4)
	2.2	14.3	
	2.2	17.8	
	2.3	17	
	2.5	20.3	
	2.4	16.8	
	2.6	21.4	
	2.4	17.6	
	2.4	17.4	
	2.1	8.7	

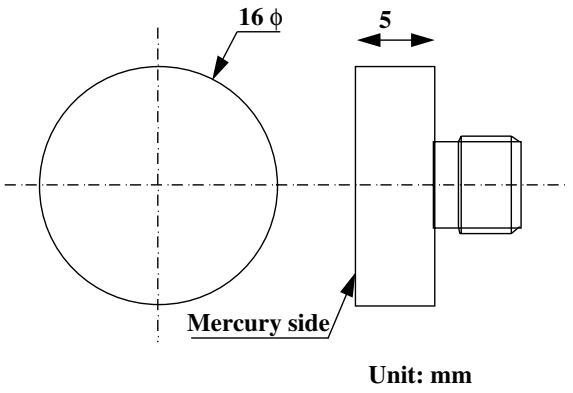

Fig. 2. Specimen geometry.

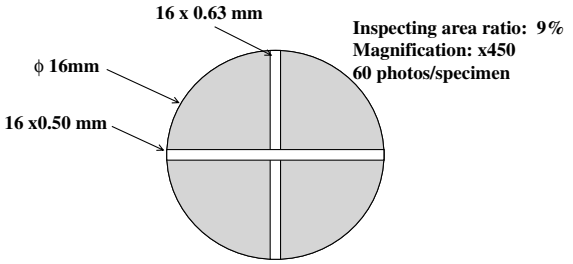

Fig. 3. Observed area before and after the test.

same microscope. SEM was used for auxiliary observation. Detailed comparison was done by using images taken from at exactly the same locations before and after the test.

Simple rules were established for interpreting observed changes when comparing before and after images. A surface change is defined as pitting except for a similar form that was seen before the examination, a change that was added at the time of the attachment or detachment of a specimen, a change due to the removal of inclusion, or the addition of a foreign substance.

3. Experimental results

3.1. Impacting tests

We controlled the air pressure of the air gun in order to change the energy of the impact bar to create design test pressure. As shown in Table 1 the realized average pressure was 84, 49, 26 and 17 MPa for cases 1, 2, 3 and 4. The actual values were larger than the scheduled ones. It must be noted that for case 4, we had one big shot: three times more than averaged value. 17 MPa is the averaged value except for the big one. Fig. 4 shows the time dependent strain measured in the input/output bars

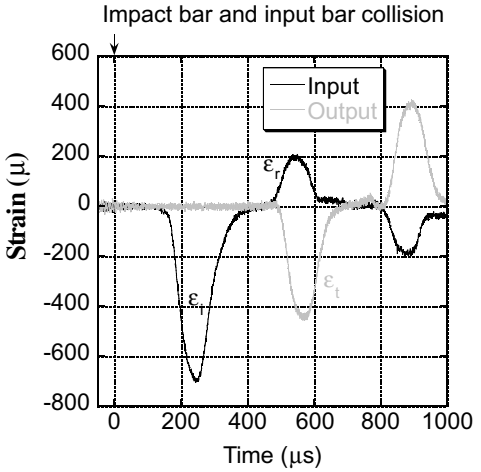

Fig. 4. Time response of the strain measured in the input/output bars.

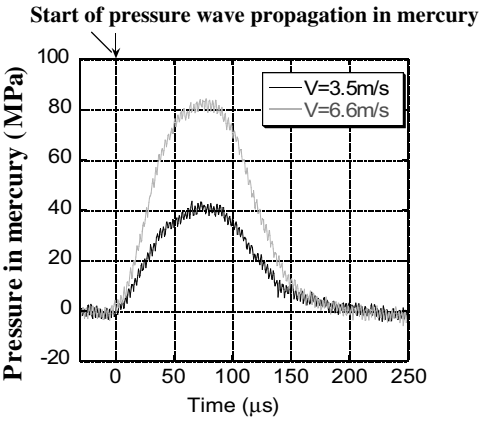

Fig. 5. Pressure response in mercury obtained by Eq. (2.10) under the conditions of $V = 6.6$ and 3.5m/s.

in the case that the impact velocity, V, is 6.6 m/s. Fig. 5 shows the pressure response in the mercury obtained by Eq. (2.10) under the condition of $V = 6.6$ and 3.5 m/s. In the case of $V = 6.6$ m/s, pressure in mercury arises up to 80 MPa at 50 μs from start of pressure wave propagation in mercury. It becomes 40 MPa in the case of $V = 3.5$ m/s.

3.2. Pitting observation

Figs. 6 and 7 show the comparison of photos before and after the tests for the case of 84 MPa average pressure in mercury. This is the case of the highest pressure among the tests. There were scratches and dots in the images easily recognized in both before and after images. However, changes could be seen in the after test.

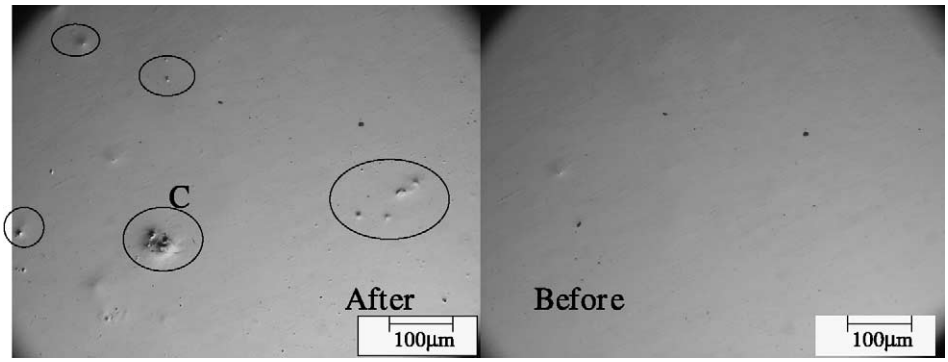

Fig. 6. Comparison of images before and after the test at 84 MPa in mercury pressure.

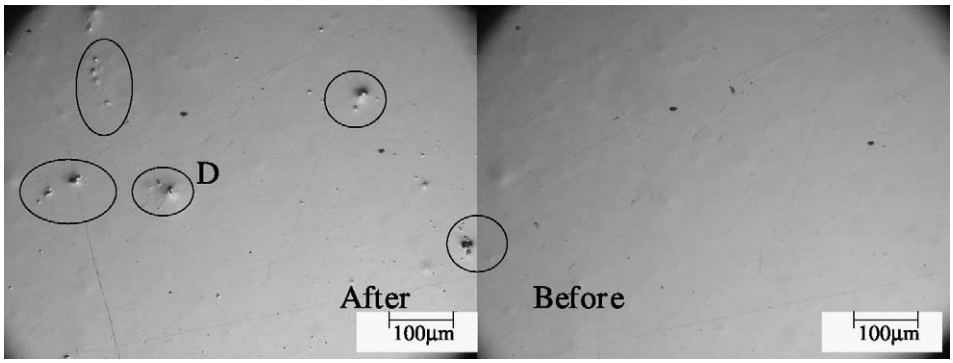

Fig. 7. Comparison of images before and after the test at 84 MPa in mercury pressure.

There are marks or dots like bombardment craters. We defined those marks as pitting. The maximum size of dotted areas is tens of μm but not over hundred μm. Pits exist isolatedly and sometimes a couple of dots exist proximately. Ten shots were given to each specimen but the number of pits is more than 10. In other words, more than one pit is generated per shot.

Fig. 8 shows the comparison of before and after photos for the case of 49 MPa average pressure. Pitting was found after the test. The size appears to be smaller than for the case of 84 MPa at least within the area covered by the inspection photos. In fact, large pits with diameter of tens of μm were found for the case of lower pressure, 26 MPa, as shown in Fig. 9. Ten shots were given to the specimen and again the number of pits is over 10.

Figs. 10 and 11 show the before and after photos for the case of average pressure 17 MPa. As mentioned

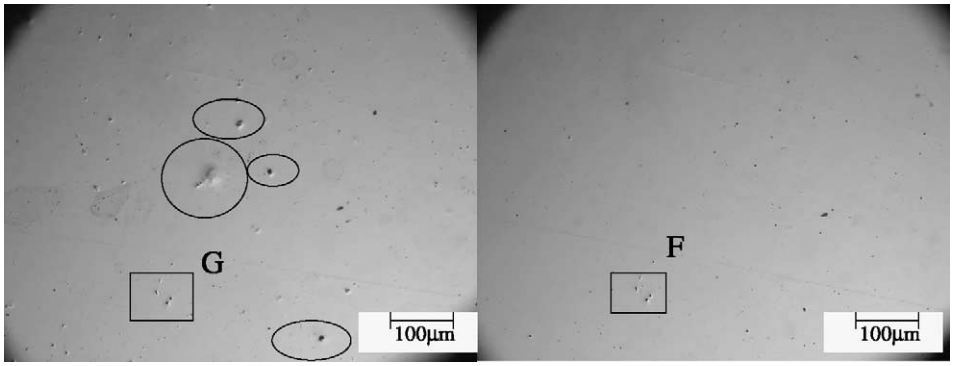

Fig. 8. Comparison of images before and after the test at 49 MPa in mercury pressure.

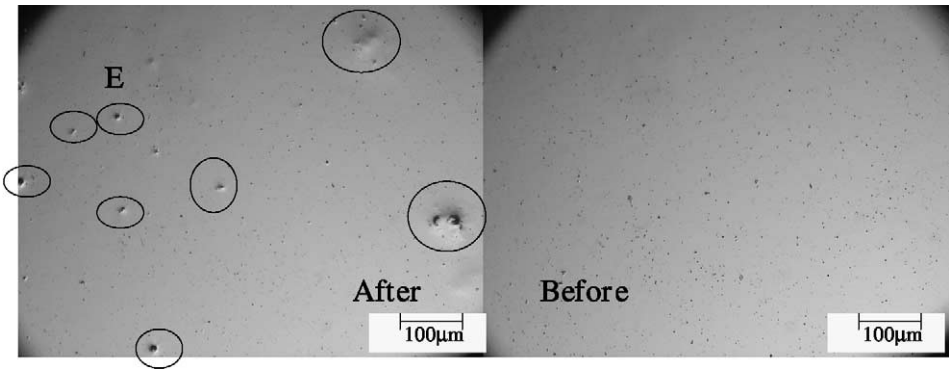

Fig. 9. Comparison of images before and after the test at 26 MPa in mercury pressure.

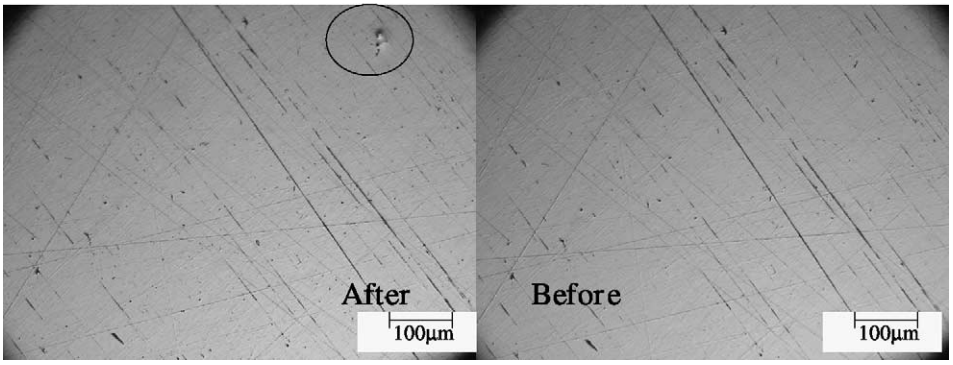

Fig. 10. Comparison of images before and after the test at 17 MPa in mercury pressure.

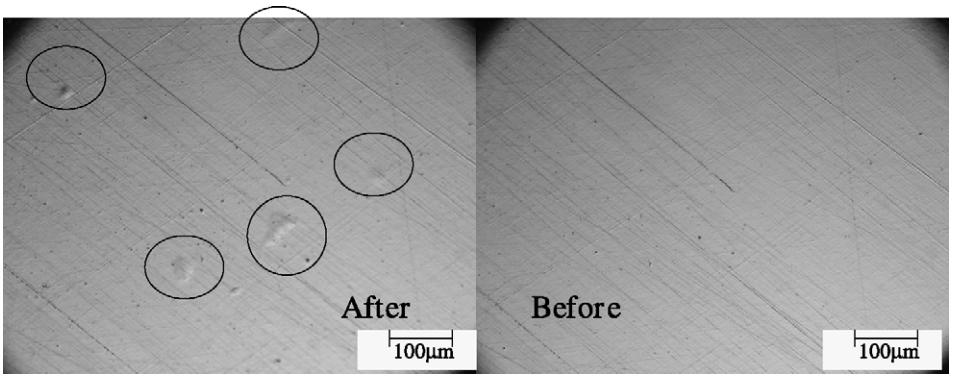

Fig. 11. Comparison of images before and after the test at 17 MPa in mercury pressure.

before, the first shot was so large that 52 MPa was applied in mercury. 17 MPa is the value of nine shots and excludes the first shot. There was a very small number of pits observed and the size of it was less than 10 μm as shown in Fig. 10. A different morphology was seen in Fig. 11. Marks observed in Fig. 11 look like shallow depressions and differ from dot shapes.

The results are summarized in Table 2. Pitting defined as morphology change between before and after tests was observed in all cases. It should be noted that the number of pitting for the case of 17 MPa averaged pressure in mercury is very limited, even if the first large shot caused all damage observed on the specimen.

Table 2
Summary of test results

Pressure in Hg, average (range) MPa	Pitting occurrence
84 (74–103)	Yes
49 (41–55)	Yes
26 (19–36)	Yes
17 (9–21, 52.2[a])	Rare

[a] One shot of 52.2 MPa was a uncontrolled case.

4. Discussion

The mechanism of pit formation is related to the pressure wave. A negative pressure in mercury generates bubbles, when pressure interferes with other waves or when the pressure expands a mercury filled target vessel. In spallation target the maximum power density is located near the target vessel. So bubbles favorite site may be near the target vessel because first the backward pressure wave changes the phase of pressure waves after inferring each other, and secondly the forward pressure wave changes the phase of pressure waves after interfering the target vessel. When bubbles collapse, a massive mercury jet flow will impinge on the target vessel and can cause pitting. The density is 13.6 g/cc in mercury and 7.8 g/cc in steel, respectively.

However, if the mercury mass flow pressure is small enough to limit deformation to the elastic regime of the material, or the mass flow pressure will work as distributed compression, the material damage will be limited and controllable during spallation target operation.

Throughout this SHPB test the test mercury pressure decreased from 84 to 17 MPa. The number of shots is only 10. There was an indication of a pressure threshold at the lowest test pressure which produced only a limited number of pits. This threshold must be proven by more than a million shots test.

In current designs of mercury spallation targets pressure in mercury is roughly 40–50 MPa [9] for megawatts of proton energy. Observation of surface morphology was studied by SEM at higher magnification for the case of 49 MPa. As mentioned in the experiment procedure, photos before test were only taken by $\times 450$ magnification. So, there was no comparison before test photos. Fig. 12 shows that there are two small holes close to each other in the center of the shallow depression with 5 μm diameter on the specimen surface taken at $\times 5000$. The size of holes is less than 1 μm.

Fig. 13 shows the other small hole at a different place with Fig. 12. The size is also less than 1 μm but a large shallow depression is not seen in the surrounding area. Fragments are scattered in the bottom of small hole. These fragments may be a collapsed inclusion like carbide which is often seen in the material. Similar changes can be found in previous figures. For example, small holes with shallow depression can be seen in the circled area C in Fig. 6 and in the circled area D in Fig. 7. The sizes of those areas are larger than the case in Fig. 12. Small hole only can be seen, for example, in circled area E of Fig. 9.

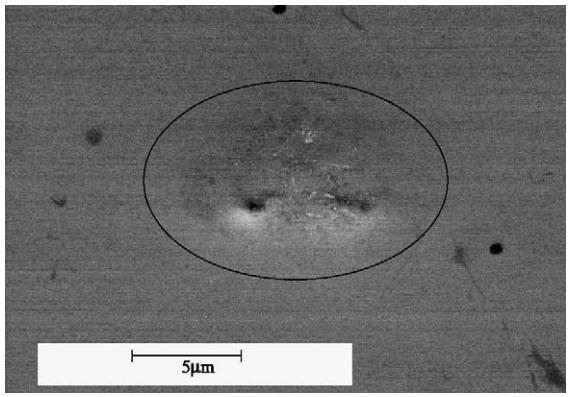

Fig. 12. Small holes in the shallow depression for the case of 49 MPa in mercury pressure.

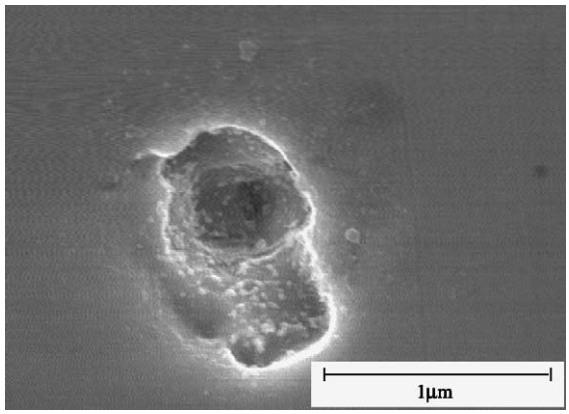

Fig. 13. Small holes for the case of 49 MPa in mercury pressure.

Nucleation site of bubbles is another interesting question for evaluating the observed pitting damage. Scratches and dot-like flaws are potential sites for nucleation of bubbles. Dot-like flaws are compared before, F, and after, G, in Fig. 8. Pitting did not occur in the rectangular area. Also there were crossed scratches in Fig. 7. Pitting was observed but not along the scratches. Scratches and dot-like flaws do not always become a nucleation site for pitting.

5. Conclusions

SHPB testing was done over a range of pressures relevant to current mercury spallation target designs. At 17 MPa average test pressure in mercury (the lowest pressure tested), the number of pits was small and damage was very limited. Although a threshold pressure

must be proven by more than a million shots test, these results suggest a threshold less than 20 MPa for 316SS. Pitting was generated at pressures over 20 MPa.

Pitting was observed but not along pre-existing scratches and dots. Scratches and dot-like flaws do not always become a nucleation sites for pitting.

Substantial damage by pitting is characterized by holes where mass is removed from the wall. A depression alone may not be substantial damage as long as it is not accompanied with holes.

References

[1] G.S. Bauer, H.Spitzer, G. von Holzen, L. Ni, J. Hastings, Proceedings of ICANS XIV, Vol. 1, 1998, p. 229.

[2] S. Ishikura, K. Kikuchi, M. Futakawa, R. Hino, Transient stress wave in a heavy liquid-metal system at high intensity proton-accelerator, ICM & M'97, 1997, p. 89.

[3] H. Kogawa, M Futakawa, S. Ishikura, K. Kikuchi, M. Kaminaga, R. Hino, Proceedings of the 3rd International WS on mercury target development, ORNL, November, 2001.

[4] B. Riemer, Proceedings of the 3rd International WS on mercury target development, ORNL, November, 2001.

[5] A. Philipp, W. Lauterborn, J. Fluid Mech. 361 (1998) 75.

[6] Y. Tomita, A. Shima, J. Fluid Mech. 169 (1986) 535.

[7] M.S. Plesset, R.B. Chapman, J. Fluid Mech. 47 (1971) 283.

[8] M. Futakawa, H. Kogawa, R. Hino, J. Phys. IV France 10 (Pr9) (2000) 237.

[9] H. Kogawa, S. Ishikura, M. Futakawa, K. Kikuchi, M. Kaminaga, R. Hino, Proceedings of ICANS XV, Vol. 2, 2001, p. 1198.